Histol Histopathol (2025) 40: 1073-1081

Histology and Histopathology
From Cell Biology to Tissue Engineering

ORIGINAL ARTICLE Open Access

USP33 promotes pulmonary microvascular endothelial cell pyroptosis by stabilizing TRAF2 through deubiquitination

Jianping Liang, Junbo Chen and Pengfei Xu

Department of Internal Medicine, Huaqiao University Hospital, Quanzhou City, Fujian Province, PR China

Summary. Objective. Inhibiting the pyroptosis of human pulmonary microvascular endothelial cells (HPMECs) is a promising therapeutic modality for acute lung injury (ALI). Given the undefined effect of ubiquitin-specific protease 33 (USP33) and tumor necrosis factor receptor-associated factor 2 (TRAF2) on pyroptosis in lung injury, this study investigates their roles in the pyroptosis of HPMECs during ALI.

Methods. The hypoxia/reoxygenation (H/R)-induced model was constructed in HPMECs. Cell viability, cytotoxicity, and cell death were determined by the cell counting kit-8 (CCK-8), Lactate dehydrogenase (LDH), and Hoechst-PI staining, respectively. Western blot and qRT-PCR were used to detect protein and gene expression levels of pyroptosis-related markers, respectively. The TRAF2 ubiquitination level was measured via immunoprecipitation.

Results. USP33 and TRAF2 expressions were elevated in H/R-induced HPMECs. Knockdown of USP33 increased cell viability and inhibited cellular pyroptosis, accompanied by decreases in IL-1β, IL-18, and Caspase-1. USP33 stabilized TRAF2 by deubiquitination. TRAF2 overexpression reversed the effect of USP33 silencing on suppressing HPMEC pyroptosis.

Conclusion. USP33 stabilizes TRAF2 by de-ubiquitination to promote HPMEC pyroptosis during ALI.

Key words: Ubiquitin-specific protease 33, Pyroptosis, Tumor necrosis factor receptor-associated factor 2, Deubiquitination, Lung injury

Corresponding Author: Jianping Liang, Department of Internal Medicine, Huaqiao University Hospital, No. 269 Chenghua North Road, Fengze District, Quanzhou City, Fujian Province, 362000, PR China. e-mail: liangjianping_ljp@163.com

www.hh.um.es. DOI: 10.14670/HH-18-835

Introduction

Acute lung injury (ALI) is a life-threatening hypoxic respiratory disease, the most severe forms of which include acute respiratory distress syndrome (ARDS) with a mortality rate of up to 40% (Bellani et al., 2016; Fan et al., 2018). ALI is characterized by the release of inflammatory factors, damage to the alveolar-capillary barrier, and acute diffuse pulmonary edema (Park et al., 2022). Human pulmonary microvascular endothelial cells (HPMECs) constitute a selective vascular barrier and are one of the main target cells attacked by reactive oxygen species in lung injury, making their injury or death an important pathological phenomenon (Wang et al., 2023). In recent years, the necessity of endothelial cell pyroptosis for the development of ALI has been confirmed (Cheng et al., 2017). Cellular pyroptosis, a cellular behavior that differs from apoptosis, mainly depends on caspase-triggered activation of downstream proteins in the cytoplasm, the formation of a cell membrane in membrane pores, and the resulting programmed cell death accompanied by cell rupture and the release of inflammatory factors (Wei et al., 2022). Increasing evidence suggests that cellular pyroptosis plays an important role in the pulmonary inflammatory response in ALI (Liu et al., 2021a; Zhou et al., 2021). Emodin can alleviate LPS-induced ALI by inhibiting the NOD-like receptor thermal protein domain associated

Abbreviations. AMPK, adenosine monophosphate-activated protein kinase; ALI, acute lung injury; ARDS, acute respiratory distress syndrome; DUB, deubiquitinating enzyme; GAPDH, glyceraldehyde-3-phosphate dehydrogenase; HPMEC, human pulmonary microvascular endothelial cell; H/R, hypoxia/reoxygenation; LDH, lactate dehydrogenase; NLRP3, NOD-like receptor thermal protein domain associated protein 3; PVDF, polyvinylidene fluoride; qRT-PCR, quantitative reverse transcription-polymerase chain reaction; SIRT1, sirtuin 1; TRAF2, tumor necrosis factor receptor-associated factor 2; Ub, Ubiquitination; ULK1, unc-51 like kinase 1; USP33, Ubiquitin-specific proteases 33; VHL, von Hippel-Lindau tumor suppressor; WB, western blot.

protein 3 (NLRP3) inflammasome-dependent pyroptosis signaling pathway *in vitro* and *in vivo* (Liu et al., 2021b), and exosomal miR-30d-5p promotes lung inflammation by enhancing M1 macrophage polarization and priming macrophage pyroptosis during ALI (Jiao et al., 2021). Therefore, inhibition of cellular pyroptosis is a promising therapeutic modality for ALI.

Ubiquitination (Ub) has emerged as a crucial mediator of signal transduction in cell death and inflammation, and the conjugation of non-degradative Ub chains produces robust signaling networks, which coordinate tissue remodeling and adaptation to tissue stress via transcriptional programs and the induction of apoptosis or necroptosis (Meier et al., 2015). Ubiquitin-specific protease 33 (USP33), a von Hippel-Lindau (VHL) (VHL tumor suppressor) protein-interacting deubiquitinating enzyme (DUB), has also been found to be involved in the deubiquitination of multiple proteins for different cellular functions (Niu et al., 2022). For example, USP33 promotes E3 ubiquitin ligase PRKN-mediated mitochondrial autophagy and inhibits neuroblastoma cell apoptosis via deubiquitination (Niu et al., 2020). USP33 also stabilizes the key regulator HIF-2α via deubiquitination in glioma stem cells in response to hypoxia (Zhang et al., 2022). Notably, USP33 expression is upregulated in the late stage of ARDS (Kong et al., 2009). However, there is a paucity of reports on the role of USP33 in ALI and how it regulates the ubiquitin-proteinase signaling pathway.

It is well known that tumor necrosis factor receptor-associated factor 2 (TRAF2) is also a ubiquitin E3 ligase, the Ub modification of which can promote lung injury and inflammation (Qian et al., 2022). Therefore, DUBs of TRAF2 may play a vital role in ALI-related research, and USP33 may be a DUB of TRAF2 that interacts to impact lung injury. USP48 of the DUB USP family has been identified as a DUB of TRAF2 (Li et al., 2018). In addition, TRAF2 can participate in programmed cell death through different pathways (Petersen et al., 2015). Reportedly (Shen et al., 2020), TRAF2 promotes necrosis by forming inflammatory complexes and mediating the Ub modification and degradation of unc-51-like kinase 1 (ULK1). Accordingly, TRAF2 is also a key factor in regulating the onset of inflammation, and pyroptosis (inflammatory cell death) is accompanied by the release of inflammatory factors. It is of great interest to fathom how TRAF2 mediates pyroptosis as a therapeutic target for ALI.

In this study, a hypoxia-reoxygenation (H/R)-induced HPMEC model was constructed to investigate the mechanism by which USP33 regulates pyroptosis in ALI and to characterize whether USP33 stabilizes TRAF2 via deubiquitination. Finally, we demonstrated that USP33 promotes pyroptosis of HPMECs by stabilizing TRAF2 via deubiquitination, thereby contributing to lung injury.

Table 1. The primer sequences of related genes.

Forward primer (5'-3')	Reverse primer (5'-3')
USP33 (human)	
GGAACTCAGCCTTCATTGCC	GTTCGAGCTAGTCCTCCACA
TRAF2 (human)	
AAGGTCTTGGAGATGGAGGC	GGCCCTTCATCACCACAAAG
GAPDH (human)	
TCGTGGAAGGACTCATGACC	CCTGCTTCACCACCTTCTTG

USP33, Ubiquitin-specific proteases 33; TRAF2, Tumor necrosis factor receptor-associated factor 2; GAPDH, Glyceraldehyde-3-phosphate dehydrogenase.

Materials and methods

H/R-induced cell models

HPMECs (AW-CELLS-H0540, Anweisci, China) were selected to construct an *in vitro* model. First, cells were cultured in RPMI-1640 medium containing 10% fetal bovine serum and 1% penicillin-streptomycin (15140122, Thermo Fisher Scientific, USA) in a humidified incubator (HIS33SD, Powers Scientific, USA) at 37°C with 5% CO_2 and 95% O_2. To fulfill the general pattern of lung ischemia-reperfusion injury, cells (5×10^4 cells/mL) were incubated for 3 h under hypoxic conditions at 37°C with 95% N_2 and 5% CO_2 in a sealed humidified incubator. After that, reoxygenation incubation was performed for 21h to collect the supernatant at 37°C with 5% CO_2 and 95% air. The percentage of O_2 was maintained at 5% under hypoxic conditions and 21% under reoxygenated conditions (Zhou et al., 2021).

Transfection

The cells were cultured in 24-well plates for 24h (1.0×10^5 cells/well). The transfection mixture containing 1.2 μL FuGENE® 6 transfection reagent (F6-1000, Neobioscience, USA), 18.8 μL OPTI-MEM (31985088, Thermo Fisher, USA) and USP33 overexpression plasmid (PPL01456-2a, PPL, China), short hairpin RNA against USP33 (shUSP33) (23032, PPL, China), TRAF2 overexpression plasmid (PPL00712-2a, PPL, China) or empty vector was immediately added and cultured with cells for 48h until the transfection efficiency analysis and induction of the H/R model.

Control HPMECs were free from treatment. HPMECs in the H/R group received H/R treatment to establish the model, while cell modeling in other groups was conducted based on transfection as required.

Quantitative reverse transcription-polymerase chain reaction (qRT-PCR) analysis

Total RNA was extracted from HPMECs using TRIzol reagent (A33251, Thermo Fisher, USA), and RNA quality was tested using NanoDrop One (840-

317400, Thermo Fisher, USA). cDNA was obtained with a cDNA synthesis kit (6210A, Takara, Japan). TB Green® Fast qPCR Mix (RR430S, Takara, Japan) was added to cDNA for qRT-PCR. The results were analyzed with a qRT-PCR instrument (V514732, Thermo Fisher, USA), calculated according to the Livak method (Livak and Schmittgen, 2001), and normalized to an internal reference glyceraldehyde-3-phosphate dehydrogenase (GAPDH). All primer sequences are summarized in Table 1.

Western blot (WB)

Proteins were isolated from HPMECs with a kit (P0028, Beyotime, China), the concentration of which was measured by the Bicinchoninic Acid (BCA) Protein Assay Kit (P0012, Beyotime, China). Thirty μg of protein was separated by electrophoresis using SDS-PAGE and then bound to a polyvinylidene fluoride (PVDF) membrane (FFP39, Beyotime, China). The membrane was blocked by 5% BSA blocking buffer, incubated first with primary antibodies overnight at 4°C (GAPDH as the endogenous control), and then with the suitable horseradish peroxidase-conjugated secondary antibody for 1h. The membrane was exposed using the enhanced chemiluminescence (ECL) reagent (P0018S, Beyotime, China), and then imaged using the BeyoImage™600 Chemiluminescent Imaging System (EI600C, Beyotime, China). Information on all antibodies is displayed in Table 2.

Cell counting kit-8 (CCK-8) assay

Cell viability was measured using a cell counting kit-8 (CCK-8) kit (C0038, Beyotime, China). A cell suspension (1×10^4) was inoculated into 96-well plates and incubated for 12h, and the incubation was continued for 1h after the addition of 10 μL CCK-8 reagent to each well. The absorbance value at 450 nm was detected by a Microplate Reader (1681135, Bio-Rad Laboratories, China).

Lactate dehydrogenase (LDH) assay

After incubation of HPMECs, proteins in the supernatant were collected for the detection of cytotoxicity employing an LDH kit (C0016, Beyotime, China). Next, 300 μL mixed reagent from the kit was added to ≥500 μL supernatant and incubated for 30 min. The absorbance value at 490-500 nm was detected by a Microplate Reader.

Hoechst-PI staining

HPMECs were incubated with Hoechst 33258 solution (1 mg/mL) for 7 min at 37°C. Cooling centrifugation was performed, and resuspension was conducted after the staining solution was discarded. Next, PI solution was added to the cells (5 mg/mL) for further incubation. Following removal of the PI solution, fixation of 10 μL cell staining solution was performed on a slide. The positive cells were viewed and photographed under a fluorescent microscope at 200× magnification. All apoptotic cells (blue fluorescence) and all PI-positive cells (red fluorescence) were counted.

Immunoprecipitation

HPMECs were cultured with Pierce IP Lysis Buffer (containing protease inhibitor) (87788, Thermo Fisher Scientific, USA), lysed at 4°C for 30 min, and centrifuged for 30 min. Lysate containing TRAF2 protein was collected and probed with primary antibody overnight at 4°C with rotation to form an immune complex. Next, the lysate and antibody (immune complex) solution were transferred to a tube containing washed magnetic bead precipitates for 20-min incubation with rotation. Pellets of magnetic beads were precipitated using a magnetic separation stand. Following resuspension, centrifugation, and heating to 95-100°C for 5 min, the pellets were precipitated using a magnetic detachment rack. The supernatant was later transferred and subjected to electrophoresis with 2 ×

Table 2. Antibodies used in this study.

Name	Catalog	Molecular weight	Dilution	Manufacturer
USP33	ab237510	107 kDa	1/1000	abcam, UK
TRAF2	ab126758	53 kDa	1/1000	abcam, UK
IL-18	ab243091	22 kDa	1/1000	abcam, UK
IL-1ß	ab254360	30 kDa	1/1000	abcam, UK
caspase-1	ab286125	45 kDa	1/1000	abcam, UK
GAPDH	ab8245	37 kDa	1/1000	abcam, UK
Ubiquitin	58395	—	1/1000	Cell signaling, USA
goat anti rabbit	31460	—	1/10000	Thermo Fisher, USA
goat anti mouse	31430	—	1/5000	Thermo Fisher, USA

USP33, Ubiquitin-specific proteases 33; TRAF2, Tumor necrosis factor receptor-associated factor 2; IL-18, Interleukin-18; IL-1ß: Interleukin-1 beta; caspase-1, Cysteine-requiring Aspartate Protease-1; GAPDH, Glyceraldehyde-3-phosphate dehydrogenase.

SDS buffer, followed by analyses in WB using a ubiquitin antibody. Information on all antibodies is displayed in Table 2.

Statistical analysis

The independent samples *t*-test was used for comparison between two groups, one-way ANOVA was used for comparison among groups, and Tukey's method was used for *post-hoc* tests. Data were described as mean ± standard deviation, which were calculated by GraphPad 8.0 (Graphpad Software Inc., CA, USA). Differences were considered statistically significant at $p<0.05$.

Results

USP33 promoted HPMEC pyroptosis during ALI

To assess whether USP33 is implicated in lung injury, we H/R induced HPMECs to construct a cell model. The results of qRT-PCR and WB showed that both mRNA and protein expressions of USP33 were upregulated in the cell model (Fig. 1A,B, $p<0.01$). To determine the role of USP33 in the process of lung injury under hypoxia, HPMECs were transfected with shUSP33, where USP33 was successfully silenced (Fig. 1C, $p<0.001$). The viability of HPMECs was reduced after modeling, while the knockdown of USP33 significantly upregulated cell viability (Fig. 1D, $p<0.001$). The elevation of LDH, another important indicator of lung injury, was also evidently suppressed by USP33 knockdown (Fig. 1E, $p<0.001$).

Hoechst-PI staining data demonstrated that the knockdown of USP33 resulted in fewer dead cells in the cell model (Fig. 2A). To further fathom the impact of USP33 on pyroptosis, the regulatory relationship between USP33 and pyroptosis-associated proteins was examined. H/R-induced upregulations of IL-1β, IL-18, and Caspase-1 were all abrogated by shUSP33 (Fig. 2B, $p<0.001$). Taken together, these results suggested that USP33 is an important regulator of lung injury and may act by promoting HPMEC pyroptosis.

USP33 interacted with TRAF2 by deubiquitinating TRAF2

To deeply explore the mechanism of USP33 in ALI, we examined TRAF2 and found its ability to participate in pyroptosis by mediating Ub. The relationships between USP33 and TRAF2 were first determined by WB. The results showed that TRAF2 levels were elevated in the cell model and were markedly downregulated after depletion of USP33 (Fig. 3A, $p<0.001$). Based on the properties of USP33 DUB, an IP assay was applied to detect how TRAF2 Ub levels changed after USP33 overexpression. Considering Figure 3B, the expression of Ub-TRAF2 was signally reduced, suggesting that USP33 was a DUB that interacted with TRAF2. In short, we found that USP33 stabilized TRAF2 by deubiquitination.

USP33 stabilized TRAF2 by deubiquitination to promote cellular pyroptosis during ALI

To further determine whether the USP33/TRAF2 axis regulates HPMEC pyroptosis during ALI, rescue experiments were designed. We transfected HPMECs with TRAF2 overexpression plasmid and obtained upregulated TRAF2 (Fig. 4A, $p<0.001$). In H/R-induced injury of HPMECs, the promotion of cell viability was significantly inhibited following transfection with

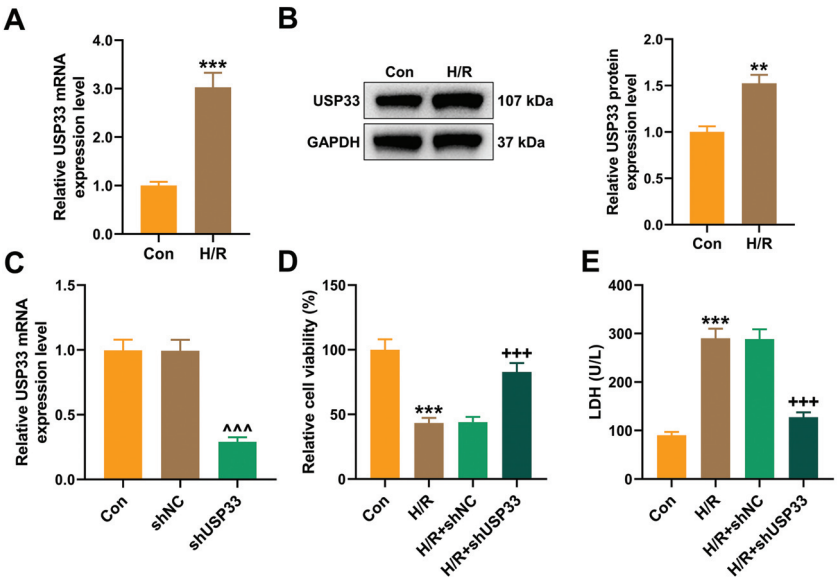

Fig. 1. USP33 was highly expressed in hypoxia-reoxygenation (H/R) cell models and the knockdown of USP33 promoted cell viability. **A.** Expression of USP33 in the H/R-induced cell model was detected by qRT-PCR **(B)** and WB. **C.** Expression of USP33 in HPMECs was detected by qRT-PCR. **D.** The relative cell viability was assessed by CCK-8. **E.** Cytotoxicity was determined by LDH. HPMECs: human pulmonary microvascular endothelial cells. qRT-PCR: Quantitative reverse transcription-polymerase chain reaction. WB: Western blot. LDH: Lactate dehydrogenase. NC: Negative control. The glyceraldehyde-3-phosphate dehydrogenase (GAPDH) was used as an endogenous control in qRT-PCR and WB. Data are presented as mean ± standard deviation. The experiments were repeated three times. $^{**}p<0.01$, $^{***}p<0.001$ vs. Con; $^{\wedge\wedge\wedge}p<0.001$ vs. shNC; $^{+++}p<0.001$ vs. H/R+shNC. (n=3 per group).

TRAF2 overexpression, in comparison with the group expressing shUSP33+NC (Fig. 4B, $p<0.01$). The downregulation of LDH was reversed following transfection with TRAF2 overexpression, in comparison with the group expressing shUSP33+NC (Fig. 4C, $p<0.001$). The same result was observed in a Hoechst-PI staining assay for detecting cell death (Fig. 4D). In addition, we found that TRAF2 overexpression reversed the effect of USP33 silencing on pyroptosis-related protein expression in the H/R-induced cell model (Fig. 4E, $p<0.001$). In conclusion, TRAF2 overexpression offset the mitigating effect of USP33 silencing on

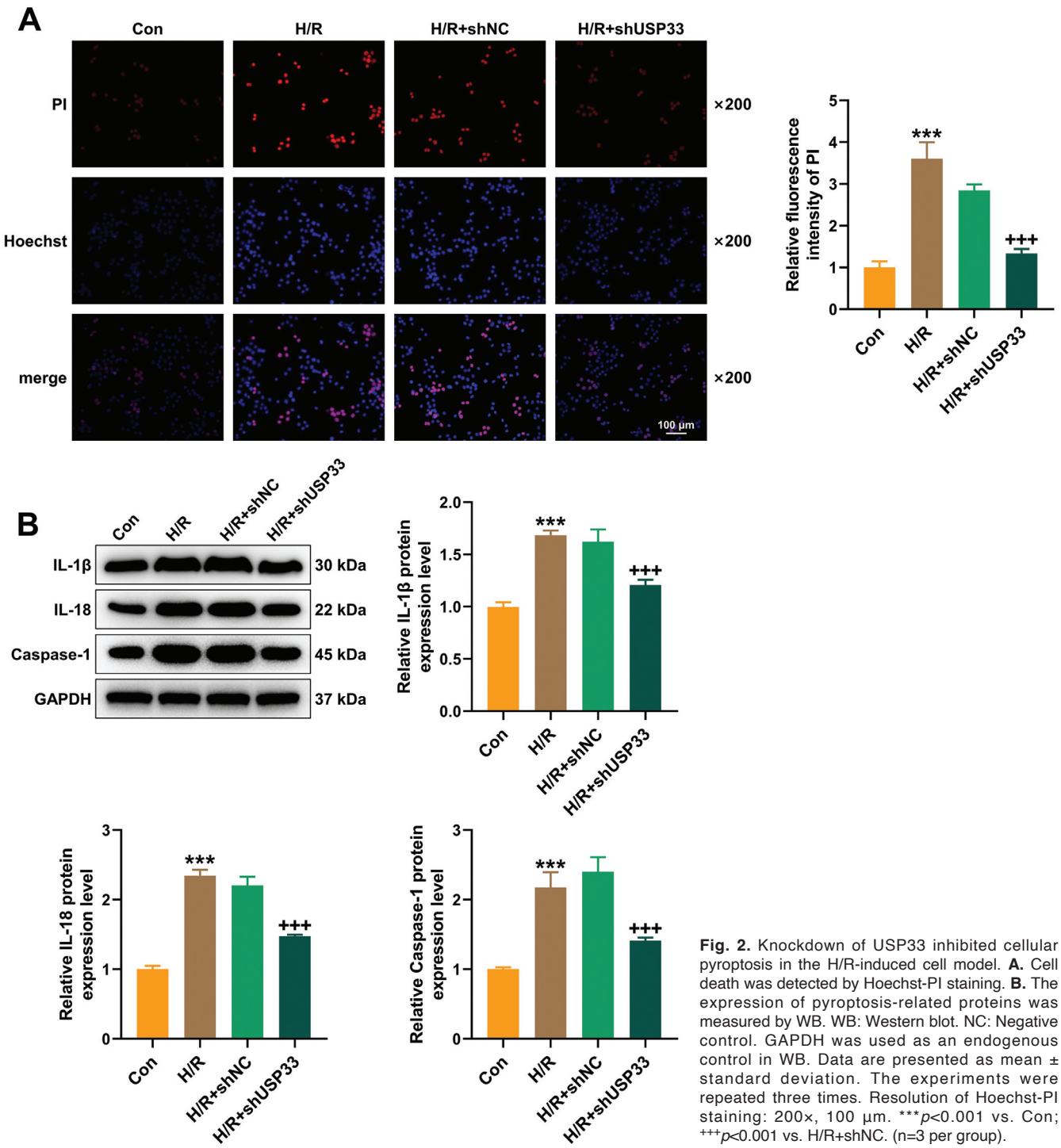

Fig. 2. Knockdown of USP33 inhibited cellular pyroptosis in the H/R-induced cell model. **A.** Cell death was detected by Hoechst-PI staining. **B.** The expression of pyroptosis-related proteins was measured by WB. WB: Western blot. NC: Negative control. GAPDH was used as an endogenous control in WB. Data are presented as mean ± standard deviation. The experiments were repeated three times. Resolution of Hoechst-PI staining: 200×, 100 μm. $^{***}p<0.001$ vs. Con; $^{+++}p<0.001$ vs. H/R+shNC. (n=3 per group).

HPMEC injury and pyroptosis.

Discussion

Numerous studies have confirmed that cell death is activated after reperfusion, leading to poor prognosis and high mortality (Fischer et al., 2000a,b). Our results also identified a promoting role of cellular pyroptosis in the development of lung injury. Meanwhile, we also detected elevated expressions of USP33 and TRAF2 in H/R-induced HPMECs and demonstrated that TRAF2 overexpression offset the effect of USP33 silencing on HPMECs. Previous studies on USP33 have focused on the field of cancer and found that USP33 can mediate the Slit-Robo signaling pathway (Wen et al., 2014), the TGF-β signaling pathway (Lu et al., 2018), and autophagy (Simicek et al., 2013). The deubiquitination modification of interacting proteins by USP33 plays a key role in numerous regulatory mechanisms.

However, the role of USP33 in pyroptosis is not well understood. We observed that USP33 silencing inhibited cellular pyroptosis, along with decreases in the pro-pyroptosis cytokines IL-1β, IL-18, and Caspase-1. Cellular pyroptosis can be activated in an inflammasome-dependent manner, with upregulation of pro-pyroptosis factors as an important hallmark (Li and Jiang, 2023). The DUB-stabilizing proteins may play an important role in inflammasome activation. A recent study describing the mechanism of inflammatory injury in the vascular endothelium revealed that DUB UCHL1 stabilizes its interacting protein by deubiquitination and that UCHL1 deletion leads to Ub and degradation of its interacting protein, which activates inflammasomes and endothelial injury (Zhu et al., 2024). Also, UCHL1 is a key regulator for inducing ALI (Epshtein et al., 2023). In our study, we similarly found that DUB USP33 promoted HPMEC pyroptosis by stabilizing its interacting protein TRAF2 through deubiquitination.

TRAF2 belongs to the TRAF family and regulates cell survival, death, and pathological stress response through Ub modifications (Miao et al., 2016; Zhang et al., 2016; Zhou et al., 2016). An existing study confirmed that allicin can inhibit TRAF2 levels and ameliorate the activation of the NLRP3 inflammasome (Nan et al., 2021). Ub modification is a highly dynamic and reversible process, and DUB can shear conjugated ubiquitin on substrate proteins to free ubiquitin, thereby reversing the regulatory effect of Ub modification (Deng et al., 2020). We have demonstrated that TRAF2 deubiquitination was instrumental in promoting HPMEC pyroptosis, coinciding with previous findings in lung injury (Ye et al., 2020). During ARDS, ubiquitin signaling and the ubiquitin-proteinase system regulate inflammatory responses and transporter protein activity (Malik et al., 2006; Vadász et al., 2012; Shabbir et al., 2023). ALI-associated muscle atrophy is also controlled by ubiquitin-mediated protease pathways (Jaitovich et al., 2015; Files et al., 2016). Reportedly, to maintain homeostasis *in vivo* during hypoxia, newly synthesized HOIL-1L promotes the Ub of Lys48 from PKCζ to protect the lung from injury (Magnani et al., 2017). Ub signaling is a reliable target for the repair and therapy of lung injury (Magnani et al., 2018).

It has been shown that TRAF2 stability is regulated by DUBs, such as USP48 (Li et al., 2018), which influence downstream immune signaling during various cellular processes. In contrast to USP48, which removes the k48 ubiquitin chain from TRAF2 to regulate its stability, various E3 ubiquitin ligases, such as cIAP-1, bind to k48 on the TRAF2 ubiquitin chain to regulate its stability (Li et al., 2002; Chen et al., 2013). In our study, USP33 reduces the Ub-protein degradation of TRAF2 by

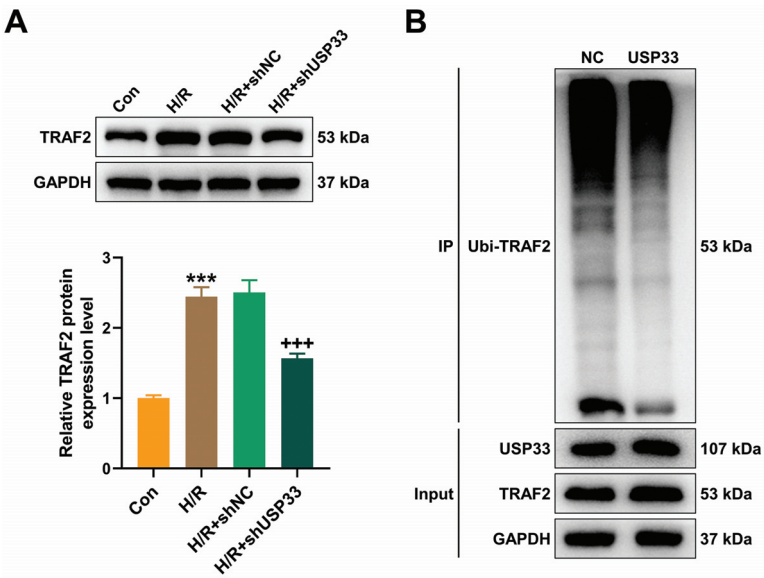

Fig. 3. USP33 interacted with TRAF2 by deubiquitination. **A.** Expression of TRAF2 in the H/R-induced cell model was determined by WB. **B.** TRAF2 ubiquitination levels were measured via IP. WB: Western blot. IP: Immunoprecipitation. NC: Negative control. GAPDH was used as an endogenous control in WB. Data are presented as mean ± standard deviation. The experiments were repeated three times. $^{***}p<0.001$ vs. Con; $^{+++}p<0.001$ vs. H/R+shNC. (n=3 per group).

deubiquitination, thereby maintaining TRAF2 stability. According to the DUB properties of USP33, we hypothesized that USP33 may be regulated by removing the k48 ubiquitin chain of lysine residues on TRAF2. In ALI, we mainly evaluated the role of the USP33/TRAF2 axis in HPMEC pyroptosis. The results showed that

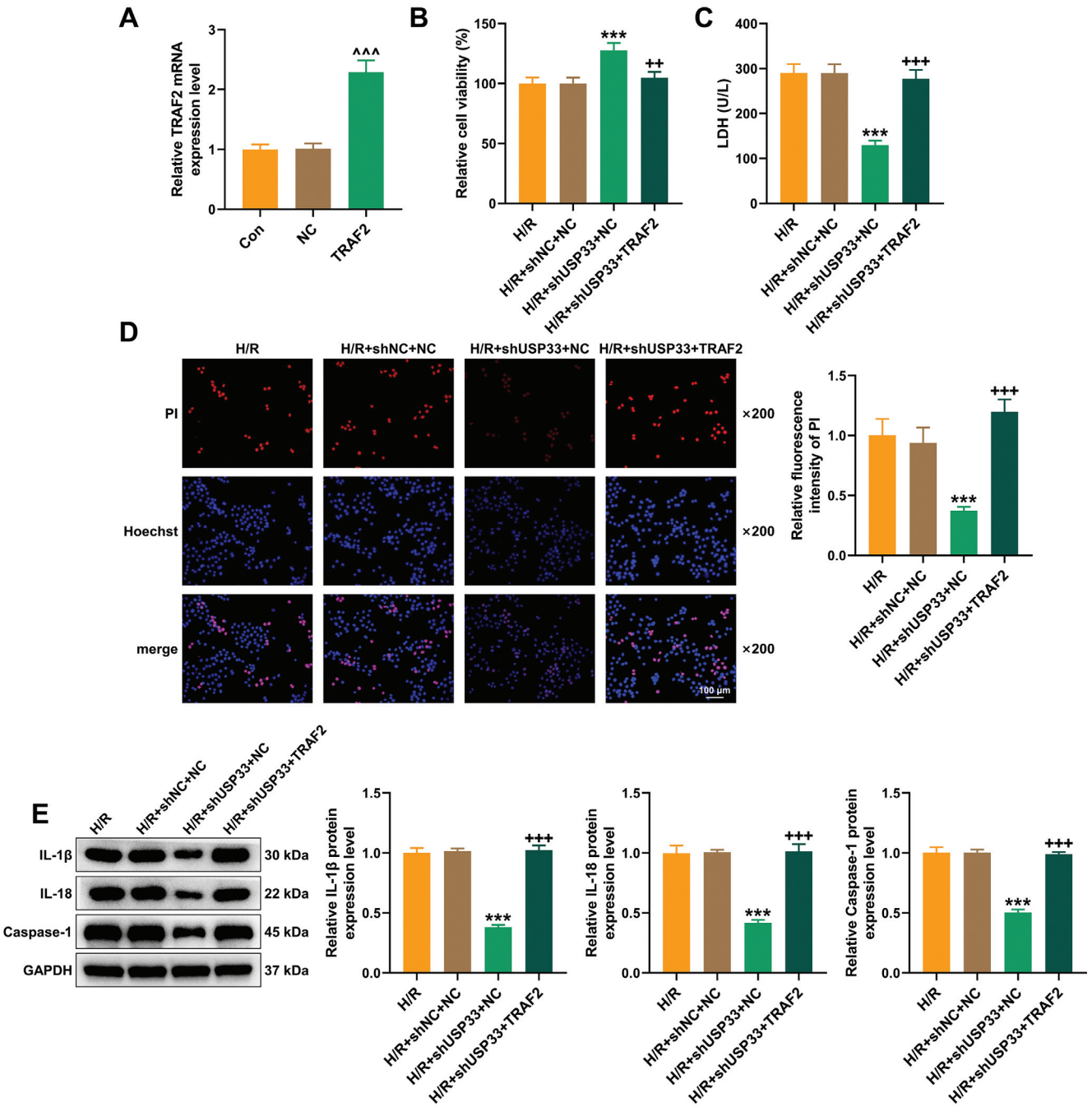

Fig. 4. TRAF2 overexpression reversed the inhibitory effect of USP33 silencing on cell injury and pyroptosis in the H/R-induced cell model. **A.** The expression of TRAF2 in HPMECs was detected by qRT-PCR. **B.** The relative cell viability was tested by CCK-8. **C.** Cytotoxicity was assessed by LDH. **D.** Cell death was detected by Hoechst-PI staining. **E.** The expression of pyroptosis-related proteins was measured by WB. qRT-PCR: Quantitative reverse transcription-polymerase chain reaction. WB: Western blot. LDH: Lactate dehydrogenase. NC: Negative control. GAPDH was used as an endogenous control in qRT-PCR and WB. Data are presented as mean ± standard deviation. The experiments were repeated three times. Resolution of Hoechst-PI staining: 200×, 100 μm. $^{\wedge\wedge\wedge}p<0.001$ vs. Con; $^{***}p<0.001$ vs. H/R+shNC+NC; $^{++}p<0.01$, $^{+++}p<0.001$ vs. H/R+shUSP33+NC. (n=3 per group).

TRAF2 overexpression reversed the inhibiting effect of USP33 knockdown on pyroptosis, evidencing that Ub/deubiquitination can regulate cell death. The present study demonstrated that USP33 promoted HPMEC pyroptosis during ALI by TRAF2 deubiquitination.

Nevertheless, our study only corroborated the role of USP33/TRAF2 in HPMEC pyroptosis by an *in vitro* model and lacked *in vivo* experimental evidence. We confirmed that USP33 was a DUB of TRAF2 by *in vitro* experiments but did not delve into the protein binding sites and Ub-dependent amino acids. In addition, the signaling pathway was not addressed in this study, which deserves to be explored deeply to discover more action targets of ALI. Finally, we need to leverage various means to detect more pyroptosis-related indicators to further study cell pyroptosis.

In conclusion, we found that USP33 and TRAF2 levels are significantly upregulated in the H/R-induced cell injury model. USP33 stabilizes TRAF2 by deubiquitination to promote HPMEC pyroptosis during ALI, suggesting that USP33 can be considered a potential therapeutic target. These findings provide valuable insights into the role of USP33 in promoting HPMEC pyroptosis via stabilization of TRAF2, and lay a strong basis for further exploration of the USP33/TRAF2 axis as a therapeutic target for ALI and related inflammatory disorders.

Acknowledgements. Not applicable.

Conflict of interest. The authors report there are no competing interests to declare.

Data availability. The analyzed data sets generated during the study are available from the corresponding author upon reasonable request.

Funding. Not applicable.

References

Bellani G., Laffey J.G., Pham T., Fan E., Brochard L., Esteban A., Gattinoni L., van Haren F., Larsson A., McAuley D.F., Ranieri M., Rubenfeld G., Thompson B.T., Wrigge H., Slutsky A.S. and Pesenti A. (2016). Epidemiology, patterns of care, and mortality for patients with acute respiratory distress syndrome in intensive care units in 50 countries. JAMA 315, 788-800.

Chen B.B., Coon T.A., Glasser J.R., McVerry B.J., Zhao J., Zhao Y., Zou C., Ellis B., Sciurba F.C., Zhang Y. and Mallampalli R.K. (2013). A combinatorial F box protein directed pathway controls TRAF adaptor stability to regulate inflammation. Nat. Immunol. 14, 470-479.

Cheng K.T., Xiong S., Ye Z., Hong Z., Di A., Tsang K.M., Gao X., An S., Mittal M., Vogel S.M., Miao E.A., Rehman J. and Malik A.B. (2017). Caspase-11-mediated endothelial pyroptosis underlies endotoxemia-induced lung injury. J. Clin. Invest. 127, 4124-4135.

Deng L., Meng T., Chen L., Wei W. and Wang P. (2020). The role of ubiquitination in tumorigenesis and targeted drug discovery. Signal Transduct. Target. Ther. 5, 11.

Epshtein Y., Mathew B., Chen W. and Jacobson J.R. (2023). UCHL1 regulates radiation lung injury via sphingosine kinase-1. Cells 12, 2405.

Fan E., Brodie D. and Slutsky A.S. (2018). Acute respiratory distress syndrome: Advances in diagnosis and treatment. JAMA 319, 698-710.

Files D.C., Ilaiwy A., Parry T.L., Gibbs K.W., Liu C., Bain J.R., Delbono O., Muehlbauer M.J. and Willis M.S. (2016). Lung injury-induced skeletal muscle wasting in aged mice is linked to alterations in long chain fatty acid metabolism. Metabolomics 12, 134.

Fischer S., Maclean A.A., Liu M., Cardella J.A., Slutsky A.S., Suga M., Moreira J.F. and Keshavjee S. (2000a). Dynamic changes in apoptotic and necrotic cell death correlate with severity of ischemia-reperfusion injury in lung transplantation. Am. J. Respir. Crit. Care Med. 162, 1932-1939.

Fischer S., Cassivi S.D., Xavier A.M., Cardella J.A., Cutz E., Edwards V., Liu M. and Keshavjee S. (2000b). Cell death in human lung transplantation: Apoptosis induction in human lungs during ischemia and after transplantation. Ann. Surg. 231, 424-431.

Jaitovich A., Angulo M., Lecuona E., Dada L.A., Welch L.C., Cheng Y., Gusarova G., Ceco E., Liu C., Shigemura M., Barreiro E., Patterson C., Nader G.A. and Sznajder J.I. (2015). High CO2 levels cause skeletal muscle atrophy via AMP-activated kinase (AMPK), FoxO3a protein, and muscle-specific ring finger protein 1 (MuRF1). J. Biol. Chem. 290, 9183-9194.

Jiao Y., Zhang T., Zhang C., Ji H., Tong X., Xia R., Wang W., Ma Z. and Shi X. (2021). Exosomal miR-30d-5p of neutrophils induces M1 macrophage polarization and primes macrophage pyroptosis in sepsis-related acute lung injury. Crit. Care 25, 356.

Jixiu F., Shulan W., Tong W., Jifang L. and Jin H. (2024). MitoQ activates the AMPK-SIRT1 pathway to inhibit pyroptosis in lung epithelial cells and alleviate sepsis-induced acute lung injury. J. Biol. Regulat. Homeostat. Agents 38, 733-743.

Kong S.L., Chui P., Lim B. and Salto-Tellez M. (2009). Elucidating the molecular physiopathology of acute respiratory distress syndrome in severe acute respiratory syndrome patients. Virus Res. 145, 260-269.

Li Y. and Jiang Q. (2023). Uncoupled pyroptosis and iL-1β secretion downstream of inflammasome signaling. Front. Immunol. 14, 1128358.

Li X., Yang Y. and Ashwell J.D. (2002). TNF-RII and c-IAP1 mediate ubiquitination and degradation of TRAF2. Nature 416, 345-347.

Li S., Wang D., Zhao J., Weathington N.M., Shang D. and Zhao Y. (2018). The deubiquitinating enzyme USP48 stabilizes TRAF2 and reduces E-cadherin-mediated adherens junctions. FASEB J. 32, 230-242.

Liu B., He R., Zhang L., Hao B., Jiang W., Wang W. and Geng Q. (2021a). Inflammatory caspases drive pyroptosis in acute lung injury. Front. Pharmacol. 12, 631256.

Liu Y., Shang L., Zhou J., Pan G., Zhou F. and Yang S. (2021b). Emodin attenuates LPS-induced acute lung injury by inhibiting NLRP3 inflammasome-dependent pyroptosis signaling pathway *in vitro* and *in vivo*. Inflammation 45, 753-767.

Livak K.J. and Schmittgen T.D. (2001). Analysis of relative gene expression data using real-time quantitative PCR and the 2(-delta delta C(T)) method. Methods 25, 402-408.

Lu J., Zhong Y., Chen J., Lin X., Lin Z., Wang N. and Lin S. (2018). Radiation enhances the epithelial- mesenchymal transition of A549 cells via miR3591-5p/USP33/PPM1A. Cell Physiol. Biochem. 50, 721-733.

Magnani N.D., Dada L.A., Queisser M.A., Brazee P.L., Welch L.C., Anekalla K.R., Zhou G., Vagin O., Misharin A.V., Budinger G.R.S.,

Iwai K., Ciechanover A.J. and Sznajder J.I. (2017). HIF and HOIL-1L-mediated PKCζ degradation stabilizes plasma membrane Na,K-ATPase to protect against hypoxia-induced lung injury. Proc. Natl. Acad. Sci. USA 114, E10178-e10186.

Magnani N.D., Dada L.A. and Sznajder J.I. (2018). Ubiquitin-proteasome signaling in lung injury. Transl. Res. 198, 29-39.

Malik B., Price S.R., Mitch W.E., Yue Q. and Eaton D.C. (2006). Regulation of epithelial sodium channels by the ubiquitin-proteasome proteolytic pathway. Am. J. Physiol. Renal Physiol. 290, F1285-1294.

Meier P., Morris O. and Broemer M. (2015). Ubiquitin-mediated regulation of cell death, inflammation, and defense of homeostasis. Curr Top Dev. Biol. 209-239.

Miao Y., Wu J. and Abraham Soman N. (2016). Ubiquitination of innate immune regulator TRAF3 orchestrates expulsion of intracellular bacteria by exocyst complex. Immunity 45, 94-105.

Nan B., Yang C., Li L., Ye H., Yan H., Wang M. and Yuan Y. (2021). Allicin alleviated acrylamide-induced NLRP3 inflammasome activation via oxidative stress and endoplasmic reticulum stress in kupffer cells and SD rats liver. Food Chem. Toxicol. 148, 111937.

Niu K., Fang H., Chen Z., Zhu Y., Tan Q., Wei D., Li Y., Balajee A.S. and Zhao Y. (2020). USP33 deubiquitinates PRKN/parkin and antagonizes its role in mitophagy. Autophagy 16, 724-734.

Niu Y., Jiang H., Yin H., Wang F., Hu R., Hu X., Peng B., Shu Y., Li Z., Chen S. and Guo F. (2022). Hepatokine ERAP1 disturbs skeletal muscle insulin sensitivity via inhibiting USP33-mediated ADRB2 deubiquitination. Diabetes 71, 921-933.

Park J.A., Crotty Alexander L.E. and Christiani D.C. (2022). Vaping and lung inflammation and injury. Annu. Rev. Physiol. 84, 611-629.

Petersen S.L., Chen T.T., Lawrence D.A., Marsters S.A., Gonzalvez F. and Ashkenazi A. (2015). TRAF2 is a biologically important necroptosis suppressor. Cell Death Differ. 22, 1846-1857.

Shabbir W., Susan Yang K.H., Dogar A.M., Isaev D. and Oz M. (2023). Probing the ubiquitination-mediated function of epithelial sodium channel in A549 cells. Curr. Mol. Pharmacol. 16, 411-418.

Shen Y., Liu W.W., Zhang X., Shi J.G., Jiang S., Zheng L., Qin Y., Liu B. and Shi J.H. (2020). TRAF3 promotes ROS production and pyroptosis by targeting ULK1 ubiquitination in macrophages. FASEB J. 34, 7144-7159.

Simicek M., Lievens S., Laga M., Guzenko D., Aushev V.N., Kalev P., Baietti M.F., Strelkov S.V., Gevaert K., Tavernier J. and Sablina A.A. (2013). The deubiquitylase USP33 discriminates between RALB functions in autophagy and innate immune response. Nat. Cell Biol. 15, 1220-1230.

Vadász I., Weiss C.H. and Sznajder J.I. (2012). Ubiquitination and proteolysis in acute lung injury. Chest 141, 763-771.

Wang Z., Guo Z., Wang X., Liao H., Chen F., Liu Y. and Wang Z. (2023). Reduning alleviates sepsis-induced acute lung injury by reducing apoptosis of pulmonary microvascular endothelial cells. Front. Immunol. 14, 1196350.

Wei T., Zhang C. and Song Y. (2022). Molecular mechanisms and roles of pyroptosis in acute lung injury. Chin. Med. J. 135, 2417-2426.

Wen P., Kong R., Liu J., Zhu L., Chen X., Li X., Nie Y., Wu K. and Wu J.Y. (2014). USP33, a new player in lung cancer, mediates slit-robo signaling. Protein Cell 5, 704-713.

Ye L., Zeng Q., Dai H., Zhang W., Wang X., Ma R., Hong X., Zhao C. and Pan L. (2020). Endoplasmic reticulum stress is involved in ventilator-induced lung injury in mice via the IRE1α-TRAF2-NF-κB pathway. Int. Immunopharmacol. 78, 106069.

Zhang X., Li C.-F., Zhang L., Wu C.-Y., Han L., Jin G., Rezaeian A.H., Han F., Liu C., Xu C., Xu X., Huang C.-Y., Tsai F.-J., Tsai C.-H., Watabe K. and Lin H.-K. (2016). TRAF6 restricts p53 mitochondrial translocation, apoptosis, and tumor suppression. Mol. Cell 64, 803-814.

Zhang A., Huang Z., Tao W., Zhai K., Wu Q., Rich J.N., Zhou W. and Bao S. (2022). USP33 deubiquitinates and stabilizes HIF2alpha to promote hypoxia response in glioma stem cells. EMBO J. 41, e109187.

Zhou Y., He C., Yan D., Liu F., Liu H., Chen J., Cao T., Zuo M., Wang P., Ge Y., Lu H., Tong Q., Qin C., Deng Y. and Ge B. (2016). The kinase CK1ε controls the antiviral immune response by phosphorylating the signaling adaptor TRAF3. Nat. Immunol. 17, 397-405.

Zhou P., Guo H., Li Y., Liu Q., Qiao X., Lu Y., Mei P.Y., Zheng Z. and Li J. (2021). Monocytes promote pyroptosis of endothelial cells during lung ischemia-reperfusion via IL-1R/NF-κB/NLRP3 signaling. Life Sci. 276, 119402.

Zhu W., Zhu W., Wang S., Liu S. and Zhang H. (2024). UCHL1 deficiency upon HCMV infection induces vascular endothelial inflammatory injury mediated by mitochondrial iron overload. Free Radic. Biol. Med. 211, 96-113.

Accepted October 17, 2024